

Supplementary Information for

**Unique Schrödinger Semimetal State in Ternary
Be₂P₃N Honeycomb Lattice**

Lingbiao Meng, Yingjuan Zhang, Shuang Ni, Bo Li and Weidong Wu

1. Computational methods for carrier mobility

Under effective mass approximation, the acoustic-phonon-limited carrier mobility (μ) for 2D materials in the deformation potential (DP) theory [Phys. Rev. 1950, 80, 72] is expressed as:

$$\mu = \frac{2e\hbar^3 C}{3k_B T (m^*)^2 E_1^2}$$

where T is the temperature and m^* is the effective mass of the carrier along the transport direction; $E_1 = \Delta v / (\Delta l / l_0)$ is the DP constant, where Δv represents the shift of band edges under proper cell compression and dilatation, l_0 is the lattice constant in the transport direction, and Δl is its deformation; $C = (\partial^2 E / \partial \delta^2) / S_0$ is the elastic modulus, where E is the total energy of the cell and δ the applied strain while S_0 is the area of the cell. The PBE functional was adopted in the estimations.

2. Table S1-S2

Table S1: Calculated bandgaps of candidate structures with Be, Mg, Zn, P and N in initial material design.

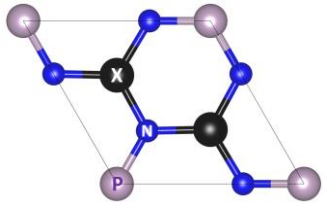
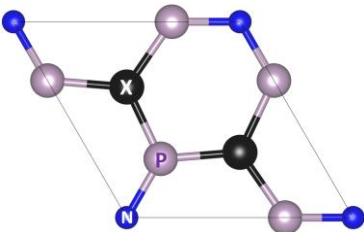
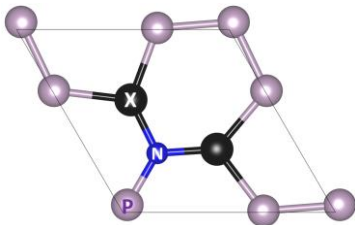
	Structure	System (X=Be, Mg, Zn)	Bandgap (eV)
C1		Be ₂ -N ₃ -P	3.850
		Mg ₂ -N ₃ -P	2.698
		Zn ₂ -N ₃ -P	2.664
C2		Be ₂ -P ₃ -N	0.000
		Mg ₂ -P ₃ -N	0.089
		Zn ₂ -P ₃ -N	0.000
C3		Be ₂ -N-P ₃	0.588
		Mg ₂ -N-P ₃	1.346
		Zn ₂ -N-P ₃	1.00

Table S2. Predicted deformation potential constant (E_1), 2D elastic modulus (C), effective mass (m^*) and mobility (μ) for electron and hole at 300 K. The vacuum level was set to zero for reference.

Carrier type	E_1 (eV)	C (N/m)	$m^*(m_e)$	$\mu(\times 10^3 \text{cm}^2/\text{V/s})$
<i>e</i>	-1.20	90	0.31	11.3
<i>h</i>	-1.65	90	-0.92	0.58

3. Figure S1-S6

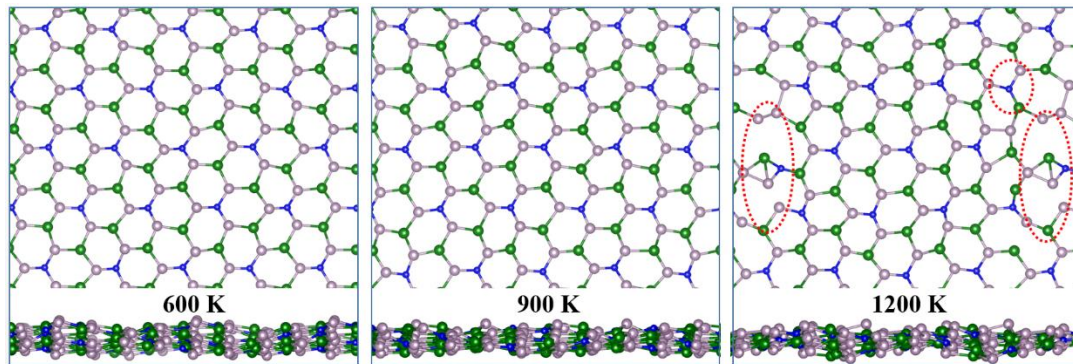


Figure S1. Snapshots of the final frame of FPMD of Be₂P₃N monolayer from 600, 900 and 1200 K (top and side views). The melted local structures at 1200 K are indicated in red-dot circles for clarity.

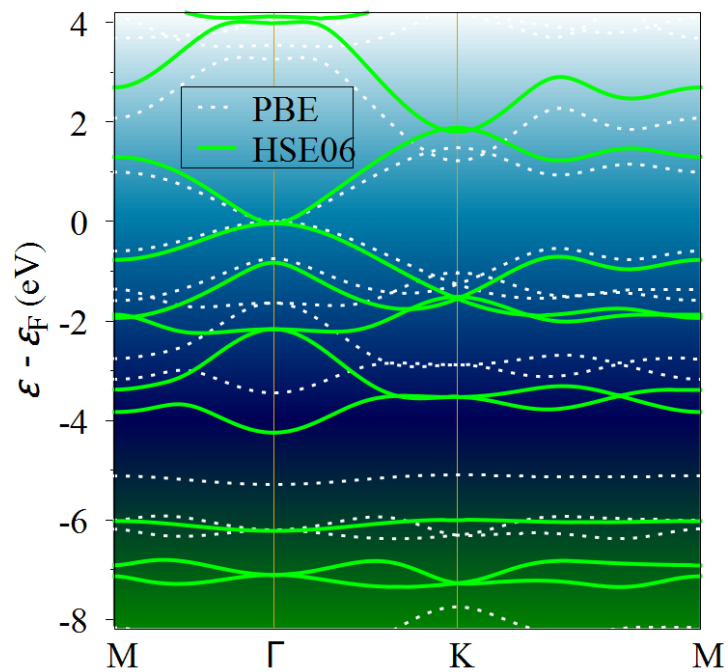


Figure S2. Band structures computed by HSE06 and PBE functionals. Note that the two functionals predict very similar band dispersions and zero bandgaps at Γ point.

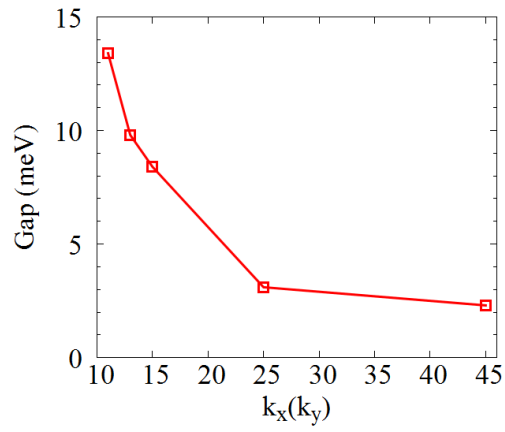


Figure S3. The SOC effect on bandgap opening calculated with different samplings of k-point density ($11 \times 11 \times 1$, $13 \times 13 \times 1$, $15 \times 15 \times 1$, $25 \times 25 \times 1$ and $45 \times 45 \times 1$). Considering the tendency, the ultimate SOC effect on bandgap opening will be further decreased, while may not be null.

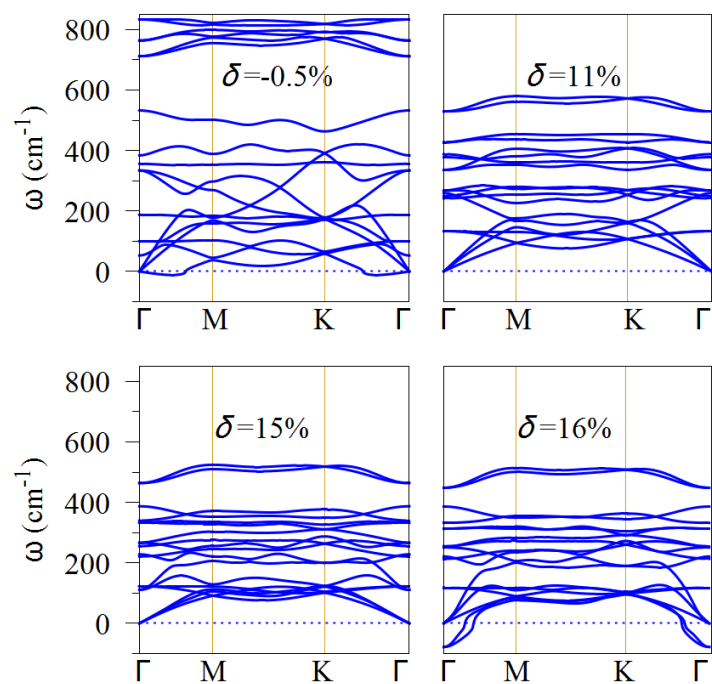


Figure S4. Phonon dispersions of Be₂P₃N monolayer under different biaxial strains.

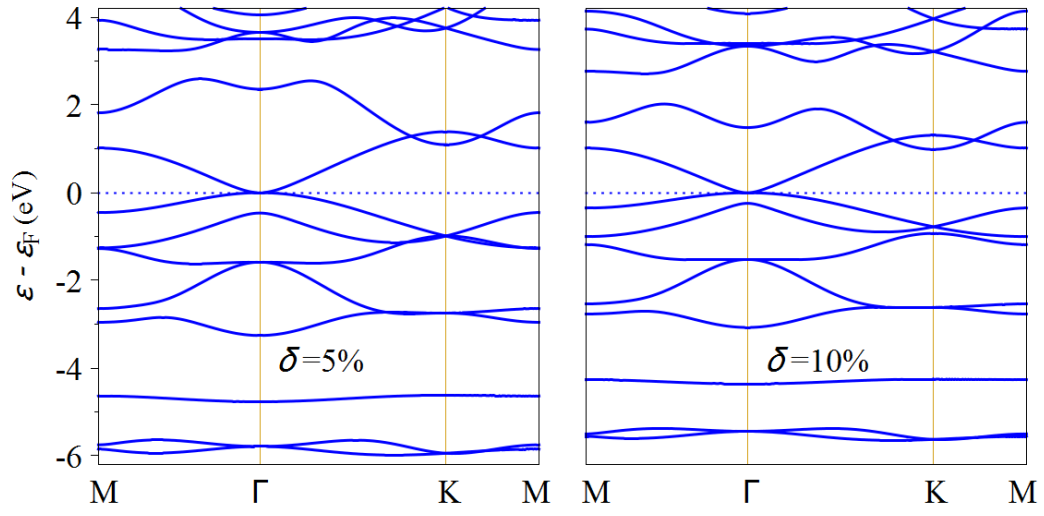


Figure S5. Band structures of Be₂P₃N monolayer under different biaxial strains.

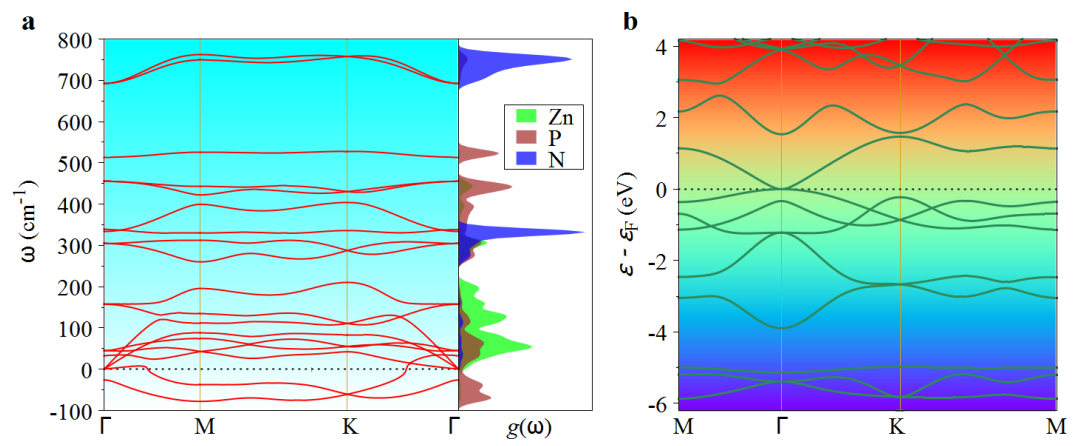


Figure S6. Phonon dispersion (a) and band structure (b) of Zn₂P₃N monolayer.